

# Assessing the Hemodynamic Influence between Multiple Lesions in a Realistic Right Coronary Artery Segment: a Computational Study

Panagiotis K. Siogkas, Antonis I. Sakellarios, Michail I. Papafaklis, Kostas A. Stefanou, Lambros M. Athanasiou, Themis P. Exarchos, Katerina K. Naka, Lampros K. Michalis and Dimitrios I. Fotiadis,  
*Senior Member IEEE*

**Abstract**— Coronary artery disease is the primary cause of morbidity and mortality worldwide. Therefore, detailed assessment of lesions in the coronary vasculature is critical in current clinical practice. Fractional flow reserve (FFR) has been proven as an efficient method for assessing the hemodynamic severity of a coronary stenosis. However, functional assessment of a coronary segment with multiple stenoses ( $\geq 2$ ) remains complex for guiding the strategy of percutaneous coronary intervention due to the hemodynamic interplay between adjacent stenoses. In this work, we created four 3-dimensional (3D) arterial models that derive from a healthy patient-specific right coronary artery segment. The initial healthy model was reconstructed using fusion of intravascular ultrasound (IVUS) and biplane angiographic patient data. The healthy 3D model presented a measured FFR value of 0.96 (pressure-wire) and a simulated FFR value of 0.98. We then created diseased models with two artificial sequential stenoses of 90% lumen area reduction or with the proximal and distal stenosis separately. We calculated the FFR value for each case: 0.65 for the case with the two stenoses, 0.73 for the case with the distal stenosis and 0.90 for the case with the proximal stenosis. This leads to the conclusion that although both stenoses had the same degree of lumen area stenosis, there was a large difference in hemodynamic severity, thereby indicating that angiographic lumen assessment by itself is often not adequate for accurate assessment of coronary lesions.

## I. INTRODUCTION

Cardiovascular diseases (CVD) is considered to be the leading cause of death globally and the number of deaths caused by CVD is expected to reach the number of 23.3 million people by 2030. Several imaging techniques that

This research project has been co-financed by the European Union (European Regional Development Fund- ERDF) and Greek national funds through the Operational Program “THESSALY- MAINLAND GREECE AND EPIRUS-2007-2013” of the National Strategic Reference Framework (NSRF 2007-2013).

P.K. Siogkas, A.I. Sakellarios, L.M. Athanasiou and D.I. Fotiadis are with the Unit of Medical Technology and Intelligent Information Systems, Dept. of Materials Science and Engineering, University of Ioannina, GR 45110 (email: [psiogkas@cc.uoi.gr](mailto:psiogkas@cc.uoi.gr), [ansakel@cc.uoi.gr](mailto:ansakel@cc.uoi.gr), [lmathanas@cc.uoi.gr](mailto:lmathanas@cc.uoi.gr), corresponding author phone: +302651008803; fax: +302651008889; e-mail: [fotiadis@cs.uoi.gr](mailto:fotiadis@cs.uoi.gr)).

M.I. Papafaklis is with the Cardiovascular Division, Brigham and Women’s Hospital, Harvard Medical School, Boston, MA 02115, USA (email: [m.papafaklis@yahoo.com](mailto:m.papafaklis@yahoo.com)).

K.A. Stefanou, T.P. Exarchos and D.I. Fotiadis are researchers in Biomedical Research Institute – FORTH, GR 45110 Ioannina, Greece (email: [kstefan@cc.uoi.gr](mailto:kstefan@cc.uoi.gr), [exarchos@cc.uoi.gr](mailto:exarchos@cc.uoi.gr), [fotiadis@cs.uoi.gr](mailto:fotiadis@cs.uoi.gr)).

K.K. Naka and L.K. Michalis are with the Michaelideion Cardiac Center, Dept. of Cardiology in Medical School, University of Ioannina, GR 45110 Ioannina, Greece (email: [anaka@cc.uoi.gr](mailto:anaka@cc.uoi.gr), [lmichalis@cc.uoi.gr](mailto:lmichalis@cc.uoi.gr)).

allow the diagnosis of coronary artery disease (CAD) are present in clinical practice. Intravascular ultrasound (IVUS), optical coherence tomography (OCT), angiography as well as other numerous imaging techniques provide an insight about the condition of the coronary vasculature.

One of the most common and effective ways to assess the functional severity of a coronary lesion is the measurement of the fractional flow reserve (FFR). FFR is defined as the maximal coronary flow in a stenosed arterial segment divided by the maximal coronary flow in the same segment if it were healthy. With the induction of hyperemia in the particular vessel, if myocardial resistances remain constant and the central venous pressure is considered to be negligible, then we can calculate the myocardial FFR which is defined as the coronary pressure distal to the stenosis divided by the coronary pressure proximal to the stenosis as it is shown in Eq. (1) [1]:

$$FFR_{myo} = P_d / P_a, \quad (1)$$

where  $P_d$  is the pressure distal to the stenosis, and  $P_a$  is the aortic pressure. Fig. 1 depicts the technique with which the FFR value is obtained in a catheterization laboratory. A pressure wire is used to capture pressure values distal and proximal to the coronary stenosis during several cardiac cycles.

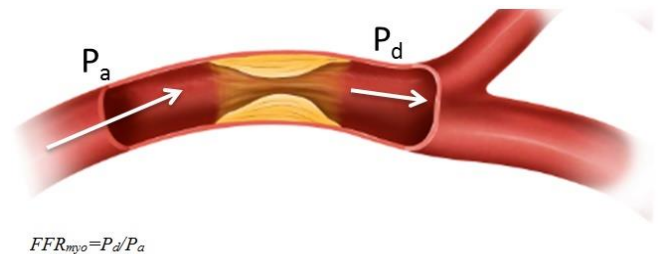


Fig. 1. Representation of the fractional flow reserve measurement procedure.

The continuous advances in computational fluid dynamics (CFD) have allowed the *in vivo* calculation of hemodynamic parameters such as pressure, endothelial shear stress and flow velocity in the coronary vasculature. However, these calculations require realistic patient-specific 3-dimensional (3D) reconstruction of the coronary vasculature. Numerous 3D reconstruction techniques have been reported in the literature. The majority of these techniques require the fusion of two imaging modalities, combining the information that is provided by the different modalities, so that accurate reconstruction of complex geometries such as bifurcations

and steep stenosis angles is performed. The most common techniques combine IVUS and biplane angiographic images [2-3], OCT and biplane angiographic images [4], or CT angiography and IVUS images [5].

A significant amount of publications regarding CFD simulations on 3D models of coronary vessels have been recently presented [6-22]. These simulations have been carried out assuming that the arterial wall is either rigid or deformable, thereby taking under consideration the interaction between the wall and the arterial lumen (Fluid Structure Interaction models-FSI). Rigid wall simulations provide useful results regarding the calculation of pressure, velocity and shear stress and require significantly lower computational time compared to FSI simulations. Conversely, FSI simulations provide more precise calculations but demand higher computational resources.

In this work, we reconstruct a healthy segment of a patient-specific right coronary artery (RCA), and additionally, we create three 3D models that include one or two artificial stenoses that cause a lumen area reduction of 90% each. One of these three models contains both stenoses, representing a diseased vessel with sequential stenosis, while the other two have only the proximal and the distal stenosis, respectively. Our aim is to investigate the hemodynamic effect of one stenosis on the other one.

## II. MATERIALS AND METHODS

### A. 3D Reconstruction

The initial 3D arterial segment was reconstructed using the following steps [3]: the end-diastolic IVUS frames were extracted from the IVUS sequence of an RCA segment of a patient. After the segmentation of the aforementioned images, the centerline of the arterial segment was extracted using an in-house developed algorithm. The borders of the arterial lumen were drawn and then the centerline was extracted from the annotated borders. Finally, the annotated end-diastolic IVUS contours were placed perpendicularly onto the generated 3D centerline estimating the relative rotational orientation of the contours, thus creating the silhouette of the 3D model. The last step of the procedure was the determination of the absolute orientation of the first IVUS frame which was performed using side branches as landmarks and backprojection on the angiographic images. Fig.2 depicts the final 3D model that was created with the aforementioned reconstruction procedure, projected on one of the two biplane angiographic images.

The initial 3D model represented a relatively healthy RCA segment which had an FFR value of 0.96 (pressure-wire), indicating the absence of inducible ischemia. Pressure and velocity values were obtained using a dedicated wire with miniaturized pressure-flow transducers at the tip (Combo wire, Volcano Corp.). The average aortic pressure of a cardiac cycle was 107.1 mmHg. In detail, this was the third cardiac cycle that was measured using the combo wire and was selected due to the fact that the signal was more stable in that cycle.

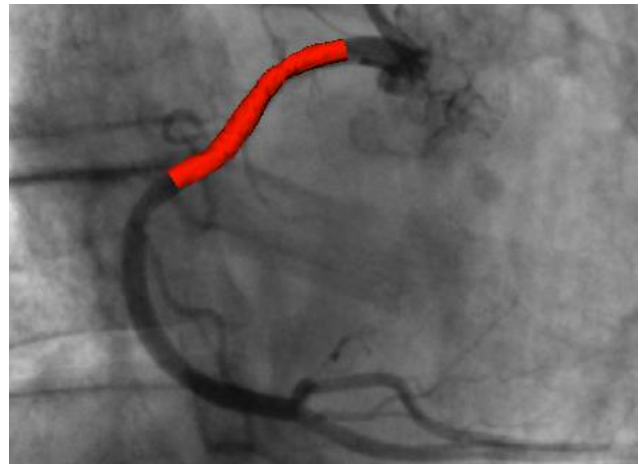


Fig 2. Final reconstructed model of the healthy case, projected on the angiographic image.

To create the 3D models that had artificial stenoses, we created an algorithm that reduces the area of the lumen by a desired percentage. In our case, we created two stenoses that reduced the lumen area by 90% (corresponding to approximately 70% diameter stenosis). The two stenoses had a distance of approximately 5.8 mm. A representation of the healthy model in transparency along with the stenosed model is depicted in Fig.3.

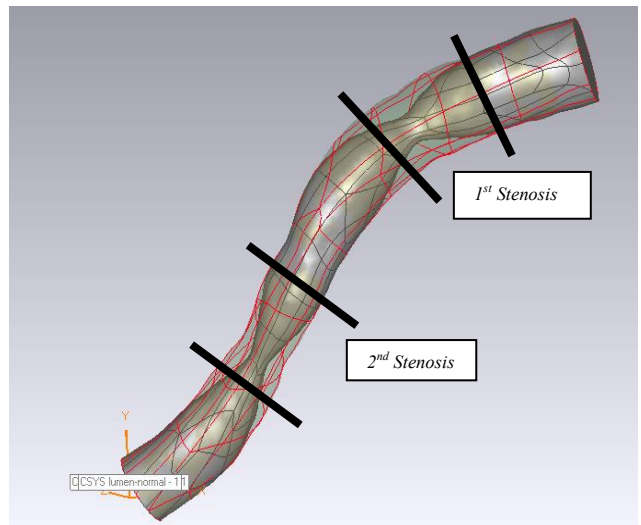


Fig 3. Transparent 3D model of the healthy RCA segment along with the solid 3D model containing both stenoses.

Then, the two stenoses are treated (i.e. restoring lumen patency) one at a time in order to determine how one affects the other in terms of pressure drop and eventually FFR values. As one can observe from the images below, when a stenosis was treated in a 3D model, the lumen would regain its original diameter as in the initial healthy model. All four 3D models are depicted in Fig.4.

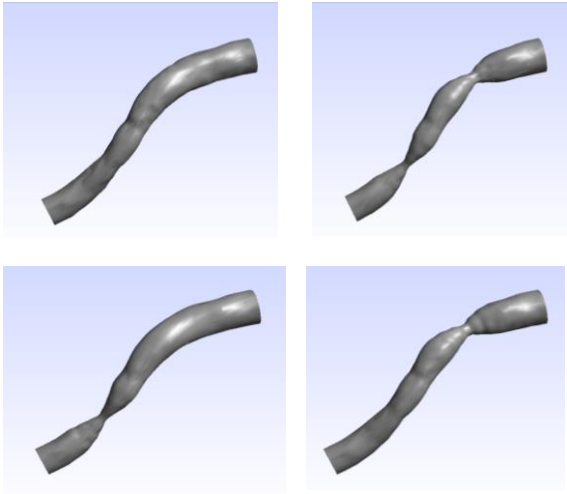


Fig 4. The healthy case of the RCA segment is depicted on the upper left image; the case including both stenoses is on the upper right image; the case with the proximal stenosis treated is depicted on the lower left image; and the case with the distal stenosis treated is on the lower right image.

## B. Blood Flow simulations

Following the reconstruction of the four 3D models, steady state blood flow simulations were carried out in each case, assuming that the arterial wall was rigid, thus not taking into account the interaction between the lumen and the arterial wall. To execute the aforementioned simulations, the Finite Element Method was used. All simulations were carried out on a Hewlett Packard Workstation with two XEON quad core processors, 24 GigaBytes of RAM and 2 Terabytes of Hard Disk storage.

### a) Rigid Wall assumption

The Navier-Stokes and the continuity equations were used to model blood flow as follows:

$$\rho \frac{\partial \mathbf{v}}{\partial t} + \rho (\mathbf{v} \cdot \nabla) \mathbf{v} - \nabla \cdot \boldsymbol{\tau} = 0, \quad (2)$$

$$\nabla \cdot (\rho \mathbf{v}) = 0, \quad (3)$$

where  $\mathbf{v}$  is the blood velocity vector,  $\rho$  is the density of blood and  $\boldsymbol{\tau}$  is the stress tensor, which is defined as:

$$\boldsymbol{\tau} = -p\boldsymbol{\delta}_{ij} + 2\mu\boldsymbol{\varepsilon}_{ij}, \quad (4)$$

where  $\boldsymbol{\delta}_{ij}$  is the Kronecker delta,  $\mu$  is the blood dynamic viscosity,  $p$  is the blood pressure and  $\boldsymbol{\varepsilon}_{ij}$  is the strain tensor calculated as:

$$\boldsymbol{\varepsilon}_{ij} = \frac{1}{2}(\nabla_i v_j + \nabla_j v_i). \quad (5)$$

Blood was treated as a Newtonian fluid having a density of 1050 kg/m<sup>3</sup> and a dynamic viscosity of 0.0035 Pa·s, and flow was considered to be laminar.

### b) Boundary Conditions

The average mass flow rate under hyperemia was applied as the inlet boundary condition in our four cases. This value was calculated using the average velocity values which were obtained by the combo wire according to the following:

$$\dot{m} = \rho \mathbf{v} \mathbf{A} \quad (6)$$

where  $\rho$  is the density of blood,  $\mathbf{v}$  is the velocity of blood and  $\mathbf{A}$  is the cross-sectional vector area. A mass flow rate of 0.0025 kg/s was used as an inlet boundary condition and was calculated using the lumen dimensions of the initial 3D model (healthy case). This value was used in all four cases so that all simulations were performed under the same boundary conditions.

An average zero-pressure value was used as an outlet boundary condition and a no-slip boundary condition was imposed on the arterial wall.

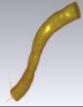
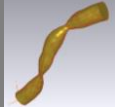

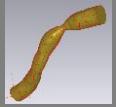
### c) Mesh

The four generated 3D models were discretized into hexahedral elements with a minimum element face size of 0.09 mm and a maximum element face size of 0.12 mm. The final discretized models contained approximately 300,000 hexahedral elements. The element size was determined after performing a mesh sensitivity analysis. The maximum number of iterations for the convergence of the solution was set as 100 and the convergence criterion was set to 10<sup>-4</sup>.

## III. RESULTS

The objective of the current work was to investigate the interplay between two stenoses of equal area reduction percentage, when only one of them is treated. The pressure gradient was calculated for each one of the four cases in order to calculate the FFR value and determine the hemodynamic severity of each case.

TABLE 1: CALCULATED PRESSURE GRADIENT AND SIMULATED FFR RESULTS FOR ALL FOUR EXAMINED CASES.

				
<b>Pressure Gradient (mmHg)</b>	2.14	37.41	29.03	10.46
<b>sFFR value</b>	0.98	0.65	0.73	0.90

Then, the calculated pressure gradient was subtracted from the value of 107.1 mmHg (i.e. the measured aortic pressure) in order to calculate the FFR value (i.e. Pd/Pa) for all four cases. Table 1 represents the pressure gradient values as well as the FFR values for all four cases.

Of note, the initial healthy case had a measured FFR value of 0.96 and a simulated FFR value (sFFR) of 0.98 indicating the validity of the used method.

#### IV. DISCUSSION

We presented a study regarding the virtual treatment of two artificial stenoses of the same area reduction percentage (90%). We used the 3D model of a realistic patient-specific healthy RCA segment which included measurements of pressure and velocity values at the distal ends of the segment. The initial healthy model exhibited a measured FFR value of 0.96 indicating that no significant stenosis was present. Three 3D models were then created including two adjacent stenoses or one single stenosis. The 3D models with one stenosis were created to simulate the effect of an angioplasty procedure restoring lumen patency. The results, showed that although both stenoses had the same percentage of area reduction, only one of them (the distal one) was hemodynamically severe since it produced an FFR value of 0.73, well below the 0.80 cut-off value indicating inducible ischemia. In contrast, when only the proximal stenosis was present, the simulated FFR value was equal to 0.90, demonstrating that despite being geometrically severe, it did not result in significant pressure drop and thus it was not hemodynamically severe. Therefore, it becomes evident that if the physician needed to choose which stenosis or stenoses to treat, he would definitely choose to treat the distal one, thereby minimizing any possible risk of complications as well as the cost of the procedure.

We are currently trying to expand the framework in which we apply the presented work, including numerous factors that affect the hemodynamic state of an arterial segment such as the number of stenoses, the percentage of area reduction, and the distance of the stenoses.

#### V. CONCLUSIONS

Our study demonstrated that even when a lumen stenosis might ostensibly seem to be of great hemodynamic significance in angiography, its potential hemodynamic effect might not be so dramatic. However, further studies on larger datasets taking into account numerous parameters need to be performed to strengthen our hypothesis.

#### REFERENCES

- [1] K. Govindarajua, I.A. Badruddina, G. N. Viswanathanb, *et al.*, "Evaluation of functional severity of coronary artery disease and fluid dynamics' influence on hemodynamic parameters: A review," *Physica Medica*, in press, 2012, doi:10.1016/j.ejmp.2012.03.008.
- [2] A. Wahle, P.M. Prause, S.C. DeJong, *et al.*, "Geometrically correct 3-D reconstruction of intravascular ultrasound images by fusion with biplane angiography--methods and validation," *IEEE Trans Med Imaging*, vol. 18(8), pp. 686-699, 1999.
- [3] C.V. Bourantas, M.I. Papafaklis, L. Athanasiou, *et al.*, "A new methodology for accurate 3-dimensional coronary artery reconstruction using routine intravascular ultrasound and angiographic data: Implications for widespread assessment of endothelial shear stress in humans," *EuroIntervention*, vol. 9(5), pp. 582-93, 2013.
- [4] L.M. Athanasiou, C.V. Bourantas, P.K. Siogkas, *et al.*, "3D reconstruction of coronary arteries using Frequency Domain Optical Coherence Tomography images and biplane angiography," *Conf Proc IEEE Eng Med Biol Soc*, vol. 2012, pp. 2647-50, 2012.
- [5] A.G. van der Giessen, M. Schaap, F.J. Gijsen, *et al.*, "3D fusion of intravascular ultrasound and coronary computed tomography for in-

vivo wall shear stress analysis: a feasibility study," *International Journal of Cardiovascular Imaging*, vol. 26(7), pp. 781-796, 2010.

- [6] F. Kabinejadian, D.N. Ghista, "Compliant model of a coupled sequential coronary arterial bypass graft: Effects of vessel wall elasticity and non-Newtonian rheology on blood flow regime and hemodynamic parameters distribution," *Medical Engineering & Phys* 34(7):860-872, 2012.
- [7] M. Malve, A. Garcia, J. Ohayon, *et al.*, "Unsteady blood flow and mass transfer of a human left coronary artery bifurcation: FSI vs. CFD," *International Communications in Heat and Mass Transfer*, vol. 39(6), pp. 745-751, 2012.
- [8] P. Vasava, P. Jalali, M. Dabagh, *et al.*, "Finite Element Modelling of Pulsatile Blood Flow in Idealized Model of Human Aortic Arch: Study of Hypotension and Hypertension," *Computational and Mathematical Methods in Medicine*, vol. 2012, Article ID 861837, 14 pages, 2012.
- [9] Md. A. Ikbala, S. Chakravartya, Sarifuddin, *et al.*, "Unsteady Analysis of Viscoelastic Blood Flow through Arterial Stenosis," *Chemical Engineering Communications*, vol. 199(1), pp. 40-62, 2012.
- [10] J.R. Leach, V.L. Rayz, M.R.K. Mofrad, *et al.* "An efficient two-stage approach for image-based FSI analysis of atherosclerotic arteries." *Biomechanics and Modeling in Mechanobiology*, vol. 9(2), pp. 213-223, 2010.
- [11] D. Bluestein, Y. Alemu, I. Avrahami, *et al.*, "Influence of microcalcifications on vulnerable plaque mechanics using FSI modeling," *Journal of Biomechanics*, vol. 41, pp. 1111-1118, 2008.
- [12] S.A. Kock, J.V. Nygaard, N. Eldrup, *et al.*, "Mechanical stresses in carotid plaques using MRI-based fluid-structure interaction models," *Journal of Biomechanics*, vol. 41(8), pp. 1651-1658, 2008.
- [13] A. Borghi, N.B. Wood, R.H. Mohiaddin, *et al.*, "Fluid-solid interaction simulation of flow and stress pattern in thoracoabdominal aneurysms: A patient-specific study," *Journal of Fluids and Structures*, vol. 24(2), pp. 270-280, 2008.
- [14] R. Torii, M. Oshima, T. Kobayashi, *et al.*, "Fluid-structure interaction modeling of a patient-specific cerebral aneurysm: influence of structural modeling," *Computational Mechanics*, vol. 43(1), pp. 151-159, 2008.
- [15] M.X. Li, J.J. Beech-Brandt, L.R. John, *et al.*, "Numerical analysis of pulsatile blood flow and vessel wall mechanics in different degrees of stenoses," *Journal of Biomechanics*, vol. 40(16), pp. 3715-3724, 2007.
- [16] B. Vahidi, and N. Fatourae, "Large deforming buoyant embolus passing through a stenotic common carotid artery: A computational simulation," *Journal of Biomechanics*, vol. 45(7), pp. 1312-1322, 2012.
- [17] S.H. Lee, H.G. Choi, and J.Y. Yoo, "Finite element simulation of blood flow in a flexible carotid artery bifurcation," *Journal of Mechanical Science and Technology*, vol. 26(5), pp. 1355-1361, 2012.
- [18] X.H. Wang, and X.Y. Li, "Fluid-structure interaction based study on the physiological factors affecting the behaviors of stented and non-stented thoracic aortic aneurysms," *Journal of Biomechanics*, vol. 44(12), pp. 2177-2184, 2011.
- [19] J. Lantz, J. Renner, and Karlsson M., "Wall Shear Stress in a Subject Specific Human Aorta - Influence of Fluid-Structure Interaction," *International Journal of Applied Mechanics*, vol. 3(4), pp. 759-778, 2011.
- [20] V. Vavourakis, Y. Papaharilaou, and J.A. Ekaterinaris, "Coupled fluid-structure interaction hemodynamics in a zero-pressure state corrected arterial geometry," *Journal of Biomechanics*, vol. 44(13), pp. 2453-2460, 2011.
- [21] E.O. Kung, A.S. Les, C.A. Figueroa, *et al.*, "In Vitro Validation of Finite Element Analysis of Blood Flow in Deformable Models," *Annals of Biomedical Engineering* 39(7): 1947-1960, 2011.
- [22] S.J. Park, J.M. Ahn, N.H. Pijls, *et al.*, "Validation of functional state of coronary tandem lesions using computational flow dynamics." *Am J Cardiol*. 110(11): 1578-84, 2012.